7-1-2015

Teleseismic P Wave Attenuation in the Upper Mantle Beneath the United States

Samantha Lynn Cafferky

Samantha Cafferky

Candidate

Earth and Planetary Sciences

Department

This thesis is approved, and it is acceptable in quality and form for publication:

Approved by the Thesis Committee:

Dr. Brandon Schamndt, Chairperson

Dr. Lindsay Lowe-Worthington

Dr. Joseph Galewsky

TELESEISMIC P WAVE ATTENUATION IN THE UPPER MANTLE BENEATH THE UNITED STATES

by

SAMANTHA L. CAFFERKY

B.S. EARTH AND PLANETARY SCIENCES, UNIVERSITY OF NEW MEXICO, 2012

THESIS

Submitted in Partial Fulfillment of the
Requirements for the Degree of

Master of Science
Earth and Planetary Sciences

The University of New Mexico
Albuquerque, New Mexico

July, 2015

DEDICATION

"I am thankful to all those who said no. Because of them, I did it myself." --Albert Einstein

For Tio, who always encouraged me to challenge my intellect and pursue education like it was going out of style.

For Dad, who taught me to focus until the final whistle and who never failed to get me excited about science and learning when I was feeling frustrated.

ACKNOWLEDGEMENTS

I would like to extend my deepest gratitude to several institutions and individuals who have made this degree and research possible.

First, I would like to thank the Department of Earth and Planetary Sciences and the University of New Mexico for providing the graduate funding that made the last two years possible. I would also like to thank the American Geophysical Union for providing funding to present my research at the annual fall meeting in 2013, allowing me to interact with many minds far greater than my own. I must extend my gratitude to the Geophysics and Atmospheric Sciences Department at Sandia National Labs for providing the internship that has given me important work experience and an environment where I could apply anything and everything I learned in school.

I would like to thank the National Science Foundation for funding the EarthScope project. The EarthScope project has providing an excellent, robust dataset that not only allows for more seismic research, but also increases the awareness of the unique scientific field. In addition, I must acknowledge the IRIS consortium for staying on top of their extensive dataset and maintaining an excellent network of willing scientists.

Progressing to professional acknowledgements, I would like to recognize my committee, without which I would not be where I am. I extend infinite gratitude to my main advisor, Dr. Brandon Schmandt. Brandon has been a walking repository of knowledge on all things seismology whose excitement for the field is contagious. In addition, he has been a remarkable inspiration to me professionally and personally. I extend sincerest gratitude to him for answering every possible question I could conceive with patience and understanding. I must also thank him for providing me the opportunity to go on amazing scientific adventures not just within the walls of Northrop Hall, but to outstanding field locations such as Mount Saint Helens. I also appreciate the endless patience he exercised with my personal choice to plan a wedding, a choice that I did not have the wisdom to put off until I finished graduate school. I also wish to thank him for putting up with my limitless list of injuries.

I would also like to thank Dr. Lindsay Lowe-Worthington, whose welcoming smile and excitement for geology continue to inspire myself and other students in the field. Dr. Joseph Galewsky has provided in-depth explanations of tough concepts and inspiration for the endless potential of career paths in the field of science.

I wish to thank my fellow students at the University of New Mexico: Rachel Price, Lauren Wheeler, Lauren Vargo, Lindsay Ross, and Ricky Bartlett. Thank you for providing a productive and exciting environment in Room 114. In addition, I would like to thank Sheri Singerling, Mark Holland, Laura Burkemper, Jonathan Lewis, Alison Santos, and James Foty. Thank you for being a part of our meetings every Wednesday night where we can put life aside for a few hours, accomplish spectacular feats, and go on exciting adventures.

Of course, I must extend my warmest gratitude to my family and friends who have done more for me than I could possibly say. Thank you for putting up with my hectic schedule and listening to me even when you did not want to. A very special and loving thank you to my husband, Jason Rogers, for standing with me through everything. Despite the stresses of grad school, weddings, and knee injuries, thank you for always standing patiently and solidly by my side. Your love and support mean the world to me. One last thank you to Socks, whose excitement for living and belly rubs puts a smile on my face no matter the day.

TELESEISMIC P WAVE ATTENUATION IN THE UPPER MANTLE BENEATH THE UNITED STATES

By

Samantha Cafferky

B.S., Earth and Planetary Sciences, University of New Mexico
M.S., Earth and Planetary Sciences, University of New Mexico

ABSTRACT

Using Mw>6, deep earthquakes that occurred between 2006 and 2015 and were recorded by EarthScope's Transportable Array, the P wave amplitude spectra were analyzed to examine seismic attenuation patterns in the upper mantle. 2.5 million inter-station P wave spectral ratios were inverted for maps of relative *t** variations across the United States in multiple frequency bands between 0.08 and 2 Hz. Broader frequency bands are associated with lower magnitude variations; however, the geographic pattern of attenuation is similar across all frequency bands, and the correlation values were >0.8. The d*t** maps from this study were compared with long period surface wave Q models [*Dalton et al.*, 2008] and upper mantle P wave velocity tomography [*Schmandt and Lin*, 2014]. The magnitude of *t** variations inverted from P wave spectra near 1 Hz is ~10x greater than predicted by long-period surface wave studies of upper mantle attenuation. This is caused by the influence of scattering for higher frequency P wave amplitude spectra. Ratios of transverse-to-vertical component spectra are used as a proxy for P wave

scattering as P wave energy loss due to scattering generally increases with frequency. The geometries between P wave amplitude spectral ratio studies and long period surface wave Q studies are largely similar. I suggest the geographic correlation results from volumes of greater than ~1 Hz scattering intensity preferentially being located in areas of higher mantle temperatures. The active tectonic structures in the western U.S. and presence of partial melts associated with widespread volcanism would cause increased elastic scattering in the same region where thin lithosphere and high mantle temperatures predict greater intrinsic attenuation. The effects of upper mantle temperature on t^* estimates can be overwhelmed by upper mantle scattering because similarly high t^* values can be found in the cratonic interior and western Cordillera. The results generally indicate that differences in teleseismic body wave spectral decay slopes are more strongly controlled by scattering than intrinsic attenuation.

1. LIST OF FIGURES

2. INTRODUCTION

The seismic component of the National Science Foundation's EarthScope program has gradually deployed seismometers across the contiguous United States. With 400 seismometers deployed at a time in the Transportable Array, about 70 km spacing, and open data access, the EarthScope project provides a unique opportunity to seismically investigate the solid Earth beneath the United States as a whole [*Feder*, 2014]. Not only does this afford opportunities to perform seismic velocity tomography across nearly an entire continent [e.g., *Schmandt and Lin*, 2014], but it also allows for the measurement of other seismic properties of the North American lithosphere and underlying mantle convection. Complementary seismic properties include measurements of seismic anisotropy [*Lin et al.*, 2011; *Liu et al.*, 2012; *Schmandt and Lin*, 2014], imaging of vertical velocity discontinuities or gradients [*Cao and Levander*, 2010; *Gilbert*, 2012; *Schmandt et al.*, 2012; *Ford et al.*, 2014], and measurements of seismic energy loss or attenuation.

Using seismic attenuation measurements in conjunction with seismic velocity measurements is more powerful and informative than using either in isolation. Seismic attenuation and velocity have complementary sensitivities to different properties of the mantle [*Dalton et al.*, 2009]. As an example, attenuation is exponentially dependent on temperature whereas velocity has a nearly linear dependence [*Romanowicz*, 1995]. Thus, using seismic attenuation and velocity can help constrain thermal and non-thermal contributions to seismic structure and mantle dynamics beneath the United States. Attenuation and seismic velocity also have different sensitivities to grain size variations and bulk and volatile composition [*Faul and Jackson*, 2005; *Dalton et al.*, 2009].

Interpretation of tomographic images is more robust if there is an attenuation study of commensurate resolution for comparison. Tomographic studies have shown seismic velocity structures that vary widely in size and can be as small as a ~100 km [*Romanowicz*, 1995; *Schmandt and Humphreys*, 2010]. Global attenuation studies show similar geographic variations but higher frequency body-wave attenuation studies typically find greater peak-to-peak variations in attenuation compared to low frequency surface wave studies [*Hwang et al.*, 2009; *Dalton et al.*, 2008]. In addition, the detail and consistency with which regional studies have been able to draw conclusions about the attenuation properties of the upper mantle lags behind the resolution achieved in seismic velocity studies. The large aperture (~3000 km) and regular spacing (~70 km) of high-quality broadband data provided by EarthScope's Transportable Array is well suited to provide new insight into seismic attenuation beneath North America and potential origins of the differences between body wave and surface wave estimates of lateral variations in upper mantle attenuation.

In this study, P wave amplitude spectra for deep earthquakes recorded by the Transportable Array are used to investigate upper mantle attenuation. The focus is within the United States because of the high station density from the EarthScope project. Large variations in attenuation are expected due to the wide range of tectonic provinces ranging from Archean cratons to active plate boundaries. The presence of these provinces predicts a broad range of upper mantle temperatures and, consequently, intrinsic attenuation. All three components of the broadband P wave data are analyzed to assess the importance of scattering and the results are compared with other global and regional attenuation studies. Comparison with other attenuation studies gives insight into the utility of different types

of data and methods for studying seismic attenuation. The results from this study are also compared to recent velocity tomography models to evaluate the importance of thermal and non-thermal contributions to upper mantle attenuation.

3. BACKGROUND

When a seismic wave propagates through Earth most of the deformation that occurs is elastic. However, some seismic wave energy is dissipated as it travels through the solid Earth, so the Earth is considered a slightly anelastic medium. In this case, dissipation of energy often occurs through transfer to heat or irrecoverable rock damage. There are four kinds of wave attenuation that occur in the Earth: geometric spreading, multipathing, scattering, and intrinsic attenuation [*Stein and Wysession*, 2003]. In the first three, the total energy in the propagating wave is conserved, making these elastic processes. In geometric spreading, the wave front energy is conserved, but it is progressively spread over a larger area and effectively attenuated upon reaching a receiver. Multipathing occurs when variations in the interior of the Earth focus and defocus the wave front, allowing the wave to look attenuated or amplified when reaching a receiver. Scattering, similar to multipathing, can be thought of as small, heterogeneous volumes in Earth breaking the wave front into smaller pieces and sending it in different directions. Thus, the energy that reaches the receiver is diminished but not the overall energy within the Earth. Intrinsic attenuation, an anelastic process where the seismic energy is actually converted to heat, is difficult to quantify separately from elastic processes but is a useful indicator of mantle properties, particularly when combined with velocity studies.

Seismic velocity tomography is the most commonly used proxy for attaining information about conditions within Earth's mantle from seismic waves. Seismic attenuation, though less commonly used, is an important and viable technique for investigating the mantle. While seismic attenuation is not typically used alone, it

improves the ability to interpret seismic velocity variations in terms of their physical origins[*Dalton et al.*, 2009]. The spatial resolution of attenuation studies has generally been coarse compared to velocity tomography, but recent improvements in broadband data coverage enable measurements of attenuation on finer scales.

Before attempting to interpret wave attenuation patterns for the upper mantle beneath the United States, it is important to understand how various physical and chemical properties of the mantle and seismic waves affect attenuation and how those properties in turn affect seismic velocity. Four basic types of mantle properties may have measurable effects on attenuation and velocity: temperature (which transitions to melt at the solidus), grain size, bulk composition, and the presence of volatiles in sub-solidus mantle [*Faul and Jackson,* 2005; *Dalton et al.*, 2009; *Karato,* 1993]. In addition, the differences in propagation mechanisms for P, S, and surface waves must be considered when comparing results from different studies [*Dalton et al.*, 2008].

2.1 Temperature and Partial Melt

Attenuation varies exponentially with temperature while seismic velocity varies relatively linearly [*Romanowicz*, 1995; *Stein and Wysession*, 2003]. Basic seismic wave propagation theory asserts that waves propagate slower in a warmer elastic solid than in a cooler material of the same composition due to reducing shear and bulk moduli. Stronger temperature sensitivity of attenuation compared to velocity has been observed in laboratory studies [*Anderson*, 1967]. Thus, as the waves propagate through the earth, one should see differences in attenuation associated with temperature that are more variant than the velocity differences. If temperatures draw near the material's solidus then additional effects must be considered. At the solidus of a material, the mantle will begin

to contain inter-granular partial melt. The effects of melt on seismic attenuation are not well known. Some studies suggest that partial melt will tend to increase attenuation and reduce velocities, but the details of those effects depend on the assumed melt geometry [*Hammond and Humphreys*, 2000] and mechanism of attenuation [*Dalton et al.*, 2009]. Overall, a small amount of partial melt in the upper mantle probably has a more readily detectable effect on seismic velocity than it does on attenuation [*Hammond and Humphreys*, 2000].

2.2 Grain Size

The association between grain size and attenuation is characterized by an inverse relationship [*Faul and Jackson*, 2005]. The influence of grain size on attenuation is interlaced with the grain boundary interactions within the mantle [*Jackson*, 2002]. Studies of the effect of grain size on attenuation and velocity suggest that an increase in grain size (from the mm scale to the cm scale) would correlate with an increase in velocity and a decrease in attenuation [*Faul and Jackson*, 2005]. Overall, the effects of grain sizes larger than 10 mm is not well understood and needs further experimental investigation [*Faul and Jackson*, 2005]. However, reduced grain sizes (mm scale) are expected in higher strain rate volumes of the mantle, suggesting that grain size has a relatively similar influence on seismic attenuation and velocity in the upper 300 km [*Faul and Jackson*, 2005].

2.3 Bulk Composition

Seismic attenuation is expected to have a lower sensitivity to bulk composition than seismic velocity [*Hwang et al.*, 2011]. Composition is a difficult property to characterize with great accuracy in terms of attenuation because its effects may be small

compared to thermal effects. Although cratonic peridotites can have varying compositions [*Lee et al.*, 2011], the scale of composition changes may be smaller than the wavelengths in common frequency studies.

2.4 Volatiles

The presence of volatiles, such as water, is expected to have a large effect on seismic attenuation. The presence of water is typically considered in terms of hydrogen-related defects in anhydrous minerals instead of the formation of hydrous minerals [*Karato*, 2003]. An example of this is the addition of hydroxide near the M2 site or two hydrogen atoms near the oxygen interstitials in olivine, a common, nominally anhydrous mantle mineral [*Anderson*, 1967; *Ingrin and Skogby*, 2000]. The presence of water enhances anelasticity, and therefore intrinsic attenuation, and reduces seismic velocity at low frequencies [*Karato*, 2003]. Volatiles such as hydrogen or carbon could also affect mantle properties by locally reducing the solidus temperature and initiating deeper melting in regions of decompression.

2.5 Seismic Wave Type

The type of seismic wave used to study attenuation is important for multiple reasons. Because of the difference between shear and compressional wave propagation patterns, the most commonly used methods for studying attenuation have different strengths and weaknesses for each wave type. For S wave or surface wave studies, both spectral ratio studies [*Hwang et al.*, 2011] and long period surface wave Q studies [*Dalton et al.*, 2008] are viable. The difficulty that arises with shear wave studies is the inability to determine what type of attenuation (elastic or anelastic) is being measured. With P wave studies, scattering should be apparent by the amount of energy present on

the transverse component of 3-component instruments. Because the P wave's strain orientation, teleseismic energy (which approaches a seismometer nearly vertical) should be present predominantly on the vertical and radial components. Anelastic attenuation will diminish the amplitude in the vertical and radial components but not transmit energy to the transverse component; only elastic attenuation mechanisms like scattering would disperse energy to other component directions and actually diminish the energy on the vertical component.

Seismic wave differences are also important when comparing the results of different studies. In order to get the most relevant comparisons, one needs to convert between P and S values. There are a couple assumptions used for the P-to-S conversion in this study. The first to assume that the value of t^*_p is equal to (t^*_s/2.25), as is appropriate for a Poisson solid [*Anderson*, 1967]. The second is based upon the frequency dependence of attenuation, particularly above 0.1 Hz [*Lekić et al.*, 2009]. The frequency dependence of relative attenuation t^* is represented by the simple power law, $t^* \propto t_0^* f^{-\alpha}$ [adapted from *Lekić et al.*, 2009]. In the case of this study, this power law coupled with the t^*_s/t^*_p can accommodate for comparisons between P and S wave studies; α is 0.27 (Figure 1) for the frequencies considered in *Dalton et al.*, 2008.

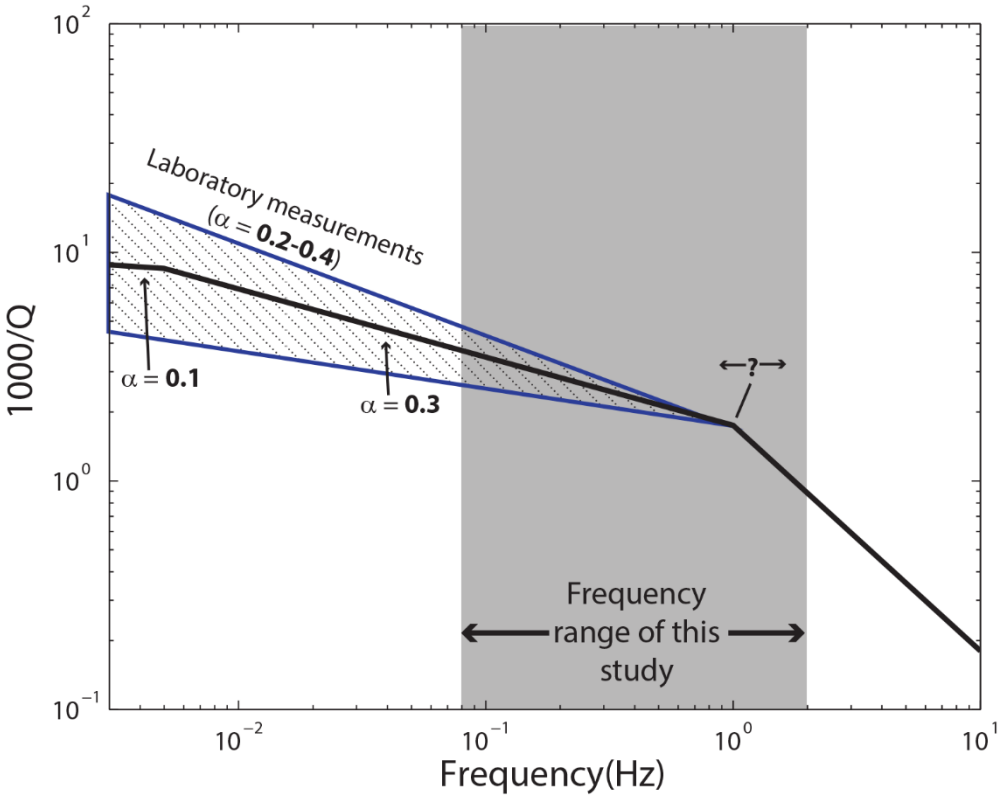

Figure 1. Illustration of exponent needed for conversion between t^*_p and t^*_s depending on frequency [adapted from *Lekić et al.*, 2009].

2.6 Previous Attenuation Studies

Within the last decade, a number of attenuation studies have been conducted to characterize mantle properties both globally and regionally. With global maps and low spatial resolution, the features that stand out in the attenuation patterns appear to be associated with temperature in the upper mantle [*Hwang et al.*, 2011]. Areas of high attenuation are correlated with tectonically active regions including rift zones and back-arc regions while low attenuation is featured in stable continental cratons [*Hwang et al.*, 2011]. This pattern is observed across much of the globe. Prior results suggest that global attenuation patterns can be explained primarily by thermal variances driven by

tectonics with some small contribution from compositional effects such as variable water content [*Dalton et al.*, 2009; *Hwang et al.*, 2011].

Few regional attenuation studies have been conducted in the United States [*Hwang et al.*, 2009], and none have been conducted using the full time range of EarthScope data. The most recent regional studies conducted in North America have low and highly variable spatial resolution with most of the instrument density in the western U.S. [*Hwang et al.*, 2009] compared to the newly available broadband seismic coverage from EarthScope. Again, the leading conclusion from these studies is that the attenuation patterns, interpreted to be intrinsic attenuation, have strong correlations with physical features in the mantle that are expected to have a strong attenuation signature (i.e. thermal changes plus some influence from water content) [*Hwang et al.*, 2009].

The United States is currently an ideal place to investigate seismic attenuation in the mantle. The EarthScope data will not only improve spatial resolution but allow more thorough evaluation of the importance of elastic and anelastic contributions to measurement of body wave amplitude spectra.

4. METHODS

The methods to be described include an enumeration of the process by which *t** values were obtained using spectral ratios from teleseismic earthquakes. The importance of different resolution length scales as well as the assumptions mentioned on page 7 are considered in order to enable comparison of *t** and prior Qs results.

The research questions investigated in this study are addressed using broadband seismic data from 2006 to 2015 obtained from the IRIS DMC (Figure 2). Attenuation in the upper mantle is analyzed using teleseismic P wave amplitude spectra, requiring a few stages of culling to determine the set of spectra used for mapping relative *t** variations across the U.S. The most basic of the selection criteria are applied to subset the possible source-receiver pairs prior to requesting data from the IRIS DMC. The focal depths of the earthquakes that are used are greater than 150 km below the surface of the Earth in order to prevent interference with direct P waves from other phases (i.e. surface reflections like *pP* and *sP*) [*Hwang et al.*, 2011]. In addition, the depth requirement eliminates attenuation by the upper mantle in the source area [*Hwang et al.*, 2011]. There is limited azimuthal coverage from deep earthquakes. As a result of the epicentral distances of 35° – 85°, most of the P waves approach the receivers nearly vertically, making resolution of *t** with depth relatively poor. Therefore, the spectra were used to invert for a map of d*t** variations averaged over the upper 300 km beneath the United States. Another important parameter when narrowing down potential earthquakes is the magnitude. Only earthquakes with estimated moment magnitudes ≥6 were used to increase the probability that the signal-to-noise ratio would be high enough to meet the additional culling criteria described below. The source-receiver pairs that meet the criteria mentioned above were

extracted from the IRIS DMC en masse and examined one earthquake at a time.

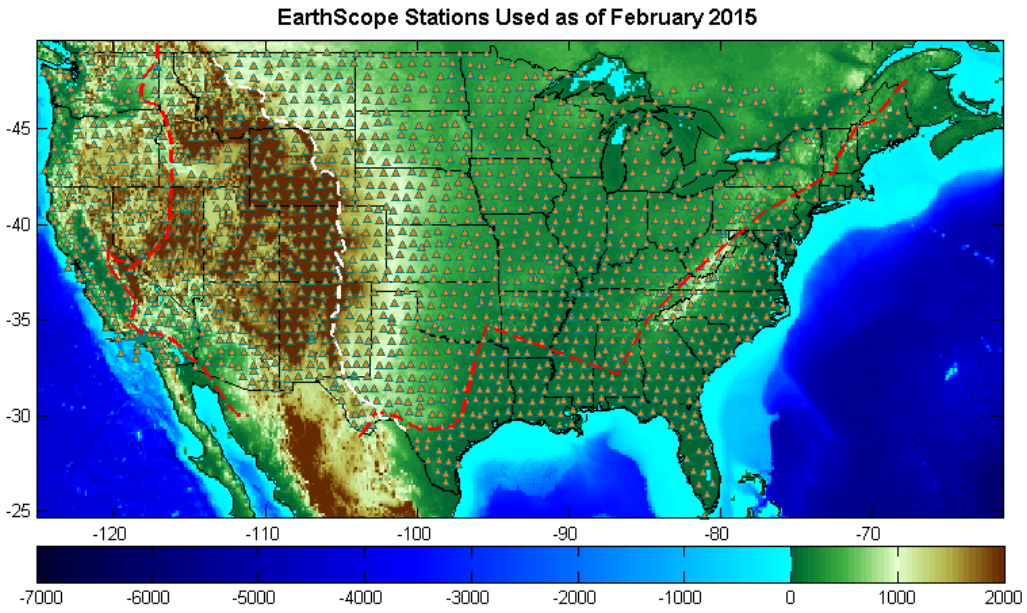

Figure 2. A map of EarthScope Transportable Array station status as of February 2015. The stations plotted are only those for which there was a high signal-to-noise deep earthquake recorded (i.e. the stations that were used for this study). Major tectonic boundaries are included as dotted white and red lines.

The need for a strong signal-to-noise ratio for each earthquake limits the total number of seismograms that are usable for this investigation. The events pulled from the IRIS DMC were examined to determine whether or not the median amplitude spectra of velocity seismograms for the event have greater power than the pre-signal noise spectra across 0.08 – 2 Hz in the vertical component (Figure 3). An earthquake was rejected if there was not enough of a difference between the median signal and pre-signal noise spectra, even if the arrival of the P wave was prominent for some stations (Figure 4). Individual stations for every event where the signal-to-noise was acceptable were examined to ensure the first arrival of the P wave was coherent (i.e. not crossing a nodal

plane within the array). Individual stations were selected using a ratio of the root-mean-square (RMS) amplitude of their 0.1 – 1 Hz signal in an interactively defined window and a pre-signal window of equal length. A minimum RMS ratio of 2.75 was considered acceptable. If an event met the selection criteria, the first arrival of the P wave was aligned using multi-channel cross-correlation of the 0.1 – 1 Hz waveforms to create a residual time map (Figure 5). These residual time shifts were used to isolate a consistent signal time window for estimation of each station's amplitude spectrum. Broader band velocity waveforms, 0.02 – 4 Hz, were subsequently used for the spectral analysis described below.

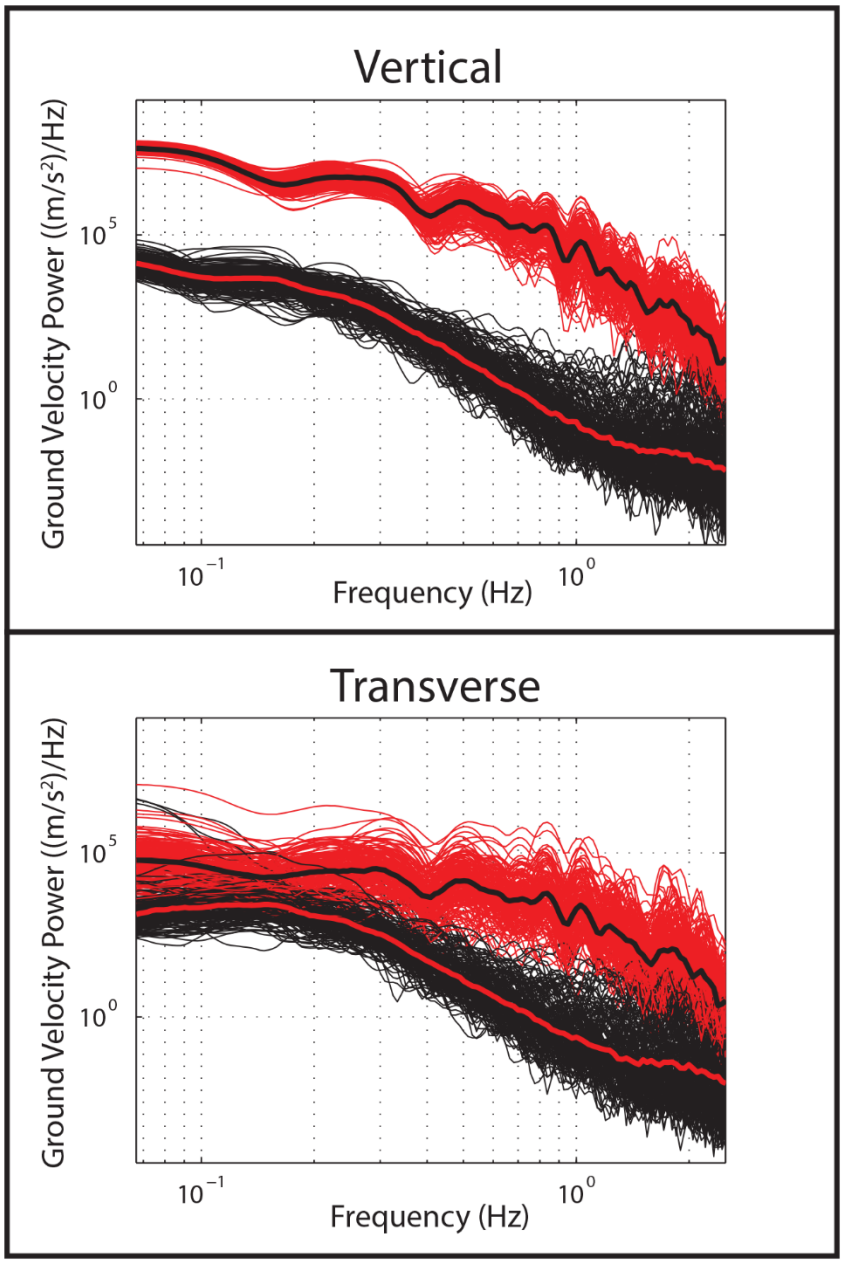

Figure 3. Amplitude spectra for the transverse and vertical components. Red is signal spectra (thick black line is median) and black is noise spectra (thick red line is median) for 2012 Colombia earthquake.

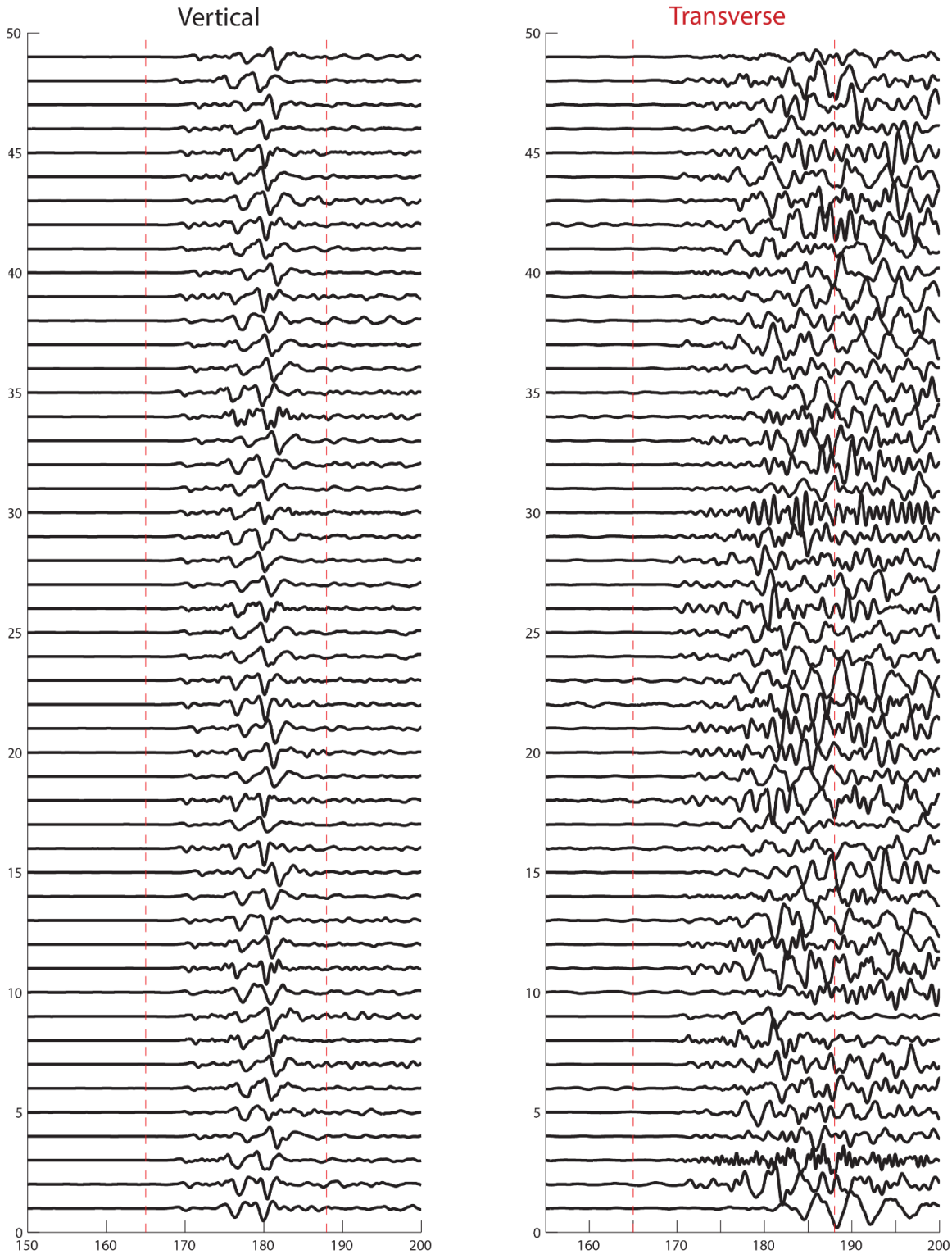

Figure 4. Vertical (left) and transverse (right) signal on a subset of stations. Incoherent energy that correlates with the arrival of energy on the vertical component is visible on the transverse component. This earthquake occurred September 30, 2012 in Colombia and had a moment magnitude of 7.2 and a depth of 170 km. This earthquake is used to

illustrate the methods process. Though the implication here is that the amplitude is the same between vertical and transverse, which is not the case. The amplitude on the transverse component is less than the amplitude on the vertical component.

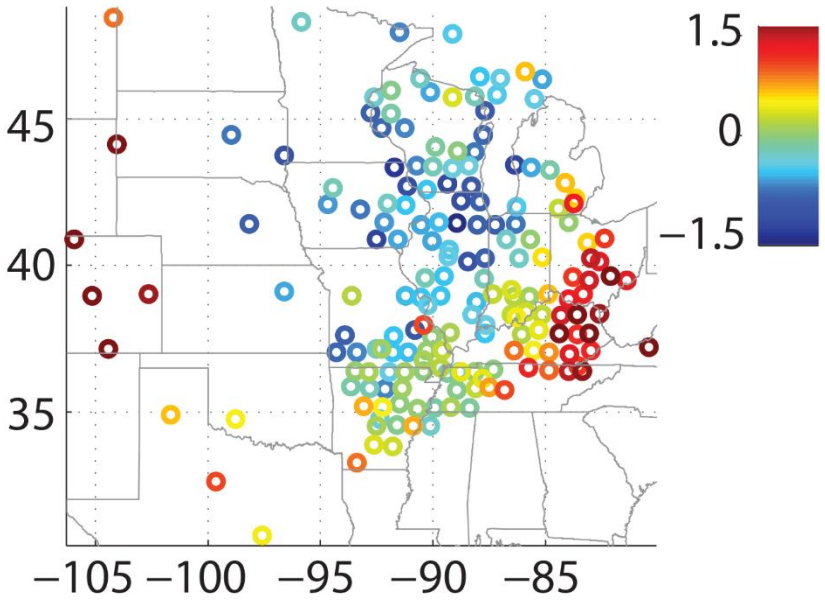

Figure 5. Residual time map after the arrival of the P wave has been aligned between all active stations.

Between 2006 and 2015, 105 earthquakes occurred within the necessary depth and magnitude parameters; overall, 44 of the events had visibly differentiated signal-to-noise ratios and an obvious P wave arrival. The locations of the events are shown in Figure 6. These events provided a total of 12,300 source-receiver pairs, which were used to invert for *t** values in four frequency bands between 0.08 and 2 Hz.

Figure 6. Global map of the 44 earthquakes used in this study.

The attenuation of teleseismic body waves is the *t** parameter defined by Stein and Wysession [2003]:

$$t^* = \int_R \frac{dt}{Q}, \quad (1)$$

where t is the travel time and Q is the quality factor, which may both vary along the ray path. Q represents the efficiency of propagation (defined as energy loss per cycle) and represents loss of energy by anelastic deformation. Apparent attenuation or observational estimates of variations in Q may arise from true anelasticity, scattering, or geometric spreading [*Hwang et al.*, 2009]. Perfectly elastic solids have infinite Q, whereas nearly elastic mediums like the solid Earth have lower, finite values. For example, Q varies from 50 – 1000 in the AK135 reference Earth model [*Kennett et al.*, 1995]. The inverse, Q^{-1}, quantifies wave attenuation. The parameter *t**, measured in seconds, is a metric of energy

loss integrated along the entire ray path for a specific source-receiver pair. When analyzing variations within a dense array at large distances (>3000 km) from the source one can assume t^* values reflect differences in structure near the receiver because the ray paths near the source are almost identical and negligible attenuation occurs in the lower mantle. Thus, in array analysis of distant earthquakes, a relative t^* value is typically estimated for each station. However, before a relative t^* value is determined, we examine a method that uses station pairs to determine the relative values of t^* from the signal-to-noise spectra.

The t^* parameter is estimated for all possible station pairs in the U.S. that recorded high signal-to-noise deep focus earthquakes between 2006 and 2015. Relative t^* between two seismic stations is estimated following *Hwang et al.*, 2009:

$$\ln\left(\frac{A_i(f)}{A_j(f)}\right) = -\pi f \Delta t^*_{p_{ij}}, \quad (2)$$

where $\frac{A_i(f)}{A_j(f)}$ is the ratio between spectra at stations *i* and *j* (Figure 7), $\Delta t^*_{p_{ij}}$ is the ratio of t^* between stations *i* and *j*, and *f* is frequency. After the stations were aligned, the spectra were estimated with a multitaper method using 9 orthogonal tapers [*Thomson*, 1982]. The time window for the signal stacks (Figure 8) was set to a fixed length of 24 seconds for an initial analysis of the data set. Only events whose signal fit within that 24-second window were used. For the second iteration through the events, the time window was adapted around the signal, between 20 and 30 seconds. This adjustment did not affect the attenuation patterns on the map nor did it increase or reduce the number of earthquakes used in the study. For the results presented in the figures, the spectra obtained with event-specific window lengths are used.

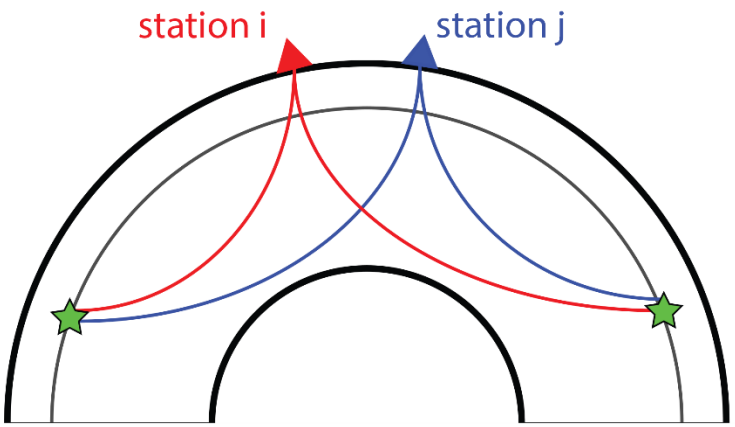

Figure 7. Raypaths of teleseismic P waves propagating from deep earthquake sources (stars) to stations (triangles) [adapted from *Hwang et al.*, 2009].

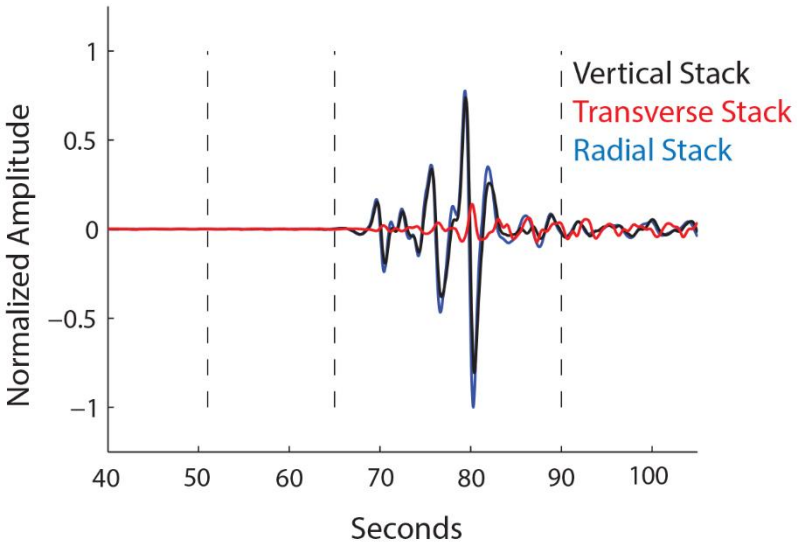

Figure 8. Median earthquake signal on vertical, transverse, radial components. P wave arrives on vertical and radial component as expected. Unexpected, incoherent energy on transverse component.

The primary benefit to using the spectral ratio (as opposed to the amplitude at a specific frequency) is that the shapes of the spectra are not as sensitive to some elastic effects such as local focusing [*Der et al.*, 1982]. The natural logarithm of the spectral ratios is fit with a best fit line using a least squares minimization (Figure 9). The slope of the best fit line provides the difference in t* values (Δt_k^*) between stations *i* and *j* [*Hwang*

et al., 2009]:

$$w\left(t_i^* - t_j^*\right) = w\Delta t_k^* \tag{3}$$

Once all the inter-station t^* estimates are obtained, an inversion is performed to find the optimal t^* value at each station across the U.S. A total of ~2.5 million inter-station t^* estimates are available for this least-squares inversion. In the inversion, the individual relative t^* estimates are weighted by their uncertainties, using the weight factor,

$$w = \exp[-(\varepsilon_k/\varepsilon_0)^2] \tag{4}$$

where ε_k is determined by the 2σ uncertainty of the best-fit slope for the inter-station spectral ratio and w reduces the weight of the measurements with the highest uncertainty, following *Hwang et al.*, 2009. The inversion also includes a parameter for each event to account for any bias associated with the movement of the Transportable Array.

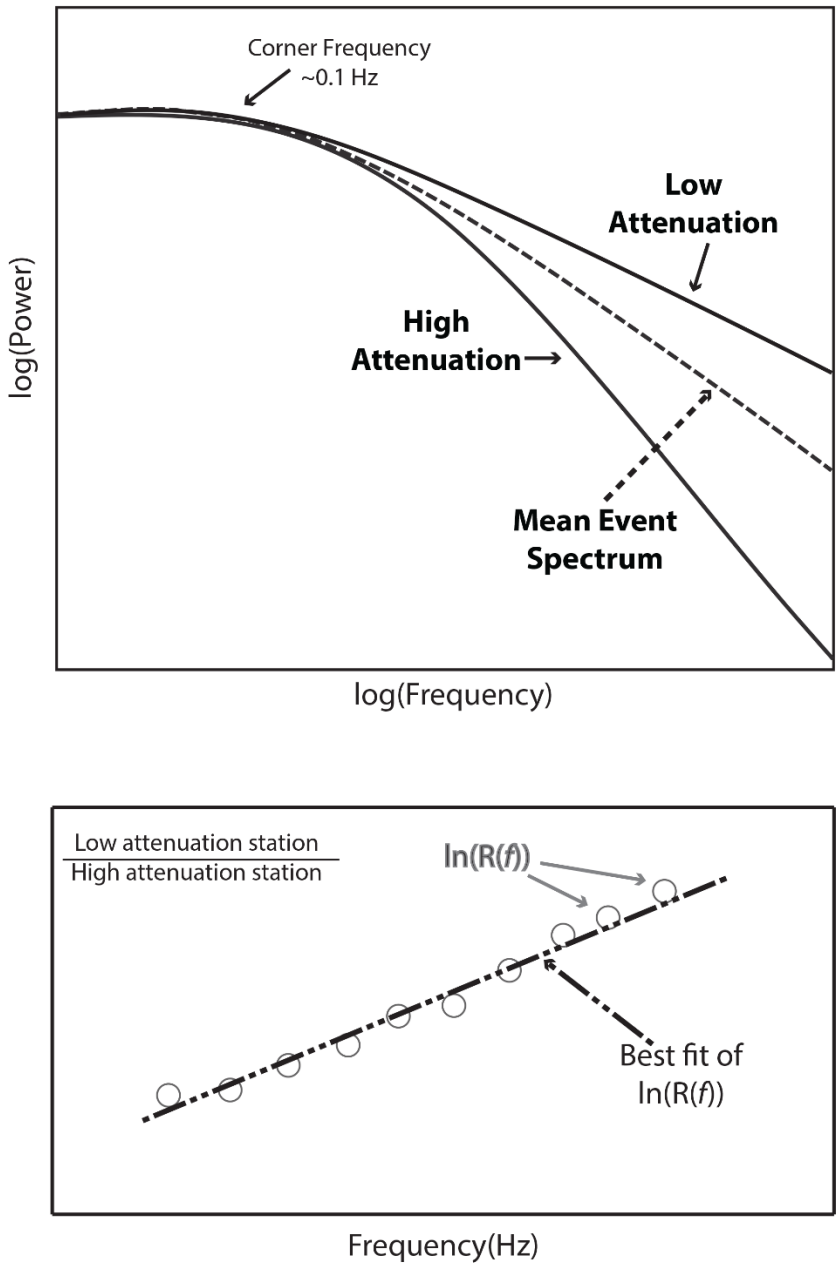

Figure 9. Top: Example power spectra from a normal earthquake, a high attenuation station, and low attenuation station. Corner frequency is ~.01- .03 Hz for earthquakes in this study. **Bottom**: $\ln(\frac{A_i(f)}{A_j(f)})$ of the low station (i)/high station (j). Relative power increases with frequency; the less attenuated spectrum decays slower causing the ratio to increase. The best fit line will get steeper with a larger difference in attenuation between the stations in a station pair.

To ensure that the variations on the map are consistent across multiple frequencies

and to discover the optimal frequency bands for accurately measuring attenuation, four bands were examined: 0.08-1 Hz, 0.08-2 Hz, 0.25-1 Hz, and 0.25-2 Hz. Weak correlation across between different frequency bands might be expected if scattering strongly affects the amplitude spectra in one or more distinct frequency bands. The resulting dt^* maps for different frequency bands are all highly correlated (>0.8) so the geometry of t^* variations appears weakly sensitive to frequencies between 0.08 – 2 Hz. However, the magnitude of t^* variations is more variable with narrower and higher frequency bands. Greater bandwidth should provide a more reliable estimate of differential attenuation, so the widest band results are preferred.

It is important to note that while the vertical component was used for choosing events, the transverse component spectrum was estimated in the same time window (Figure 4, Figure 3, Figure 8). The purpose of using the transverse component is to detect how much energy is arriving outside of the vertical-radial plane. Ideally, there would be very little or no energy on the transverse component with the arrival of the P wave in the absence of scattering due to 3-D structure or anisotropy. Typically P wave energy was visible not only on the radial and vertical components, but also on the transverse component (Figure 4). The energy on the transverse component is relatively incoherent across different stations so a stack of the transverse traces shows little power compared to radial and vertical stacks, but individual traces have high signal to noise on the transverse component (Figure 8). These characteristics are consistent with scattering due to laterally variable structure as the origin of the energy on the transverse component at the time of the P wave.

5. RESULTS

Testing different frequency bands between 0.08 and 2 Hz shows the same pattern of relative t^* but with variable amplitude. The greatest amplitude attenuation variations across the U.S. were visible in the 0.08 – 1 Hz frequency band. The difference between the 0.08 – 1 Hz band and the 0.25-1 Hz band is almost imperceptible (Figure 10). The peak-to-peak amplitude variations within the 0.08 – 2 Hz and 0.25 – 2 Hz bands are smaller compared to the other two narrower frequency bands. Comparison of the dt^* maps show that the geometries are similar across all of the frequency bands. For a more precise approach to evaluating the variations between the frequency bands, the t^* values from each frequency band were compared using their correlation values (Figure 11). The correlation values between the various bands are all greater than 0.8. Slope estimates for $ln\left(\frac{A_i(f)}{A_{j(f)}}\right)$ will be more robust and have less uncertainty for broader frequency bands. Thus, the 0.08 – 2Hz frequency band will be used for further discussion and comparison.

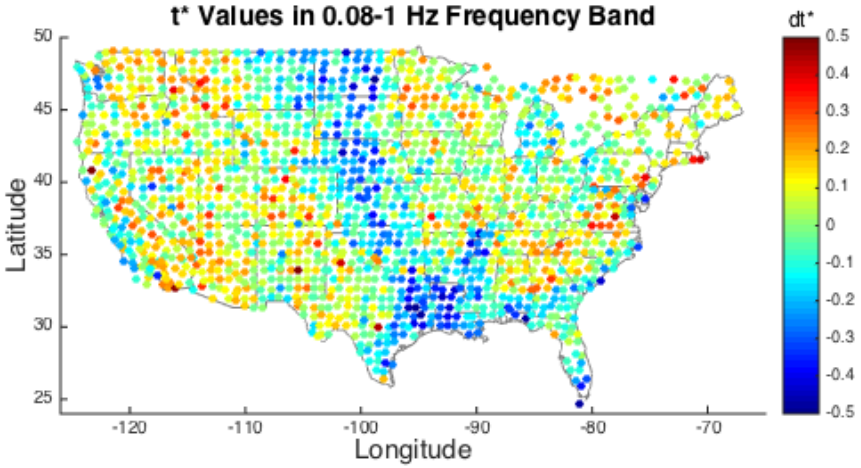
t* Values in 0.08-1 Hz Frequency Band
dt*
0.5
0.4
0.3
0.2
0.1
0
-0.1
-0.2
-0.3
-0.4
-0.5
Latitude
50
45
40
35
30
25
-120
-110
-100
-90
-80
-70
Longitude

(a)

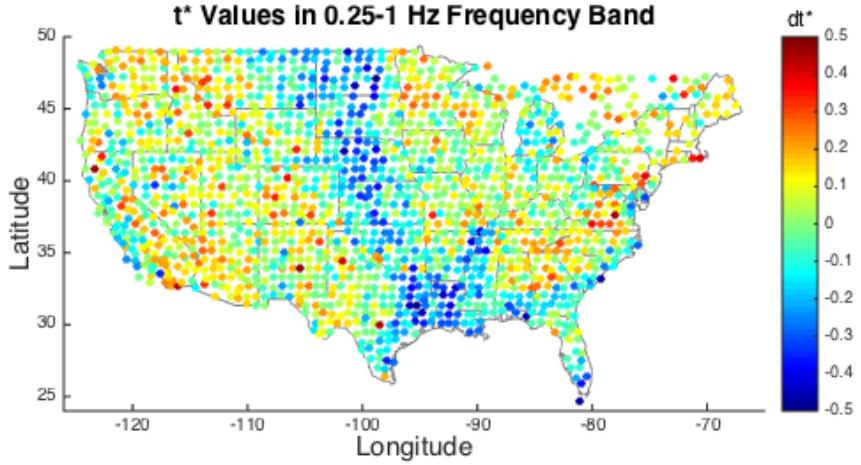
t* Values in 0.25-1 Hz Frequency Band
dt*
0.5
0.4
0.3
0.2
0.1
0
-0.1
-0.2
-0.3
-0.4
-0.5
Latitude
50
45
40
35
30
25
-120
-110
-100
-90
-80
-70
Longitude

(b)

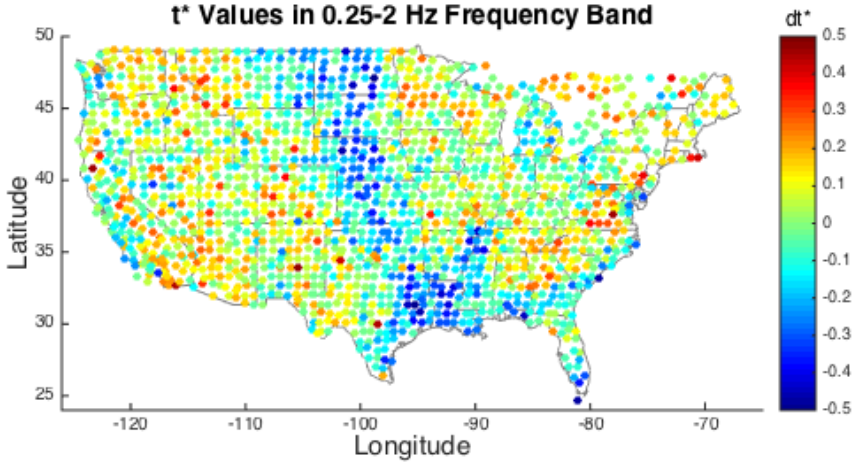
t* Values in 0.25-2 Hz Frequency Band
dt*
0.5
0.4
0.3
0.2
0.1
0
-0.1
-0.2
-0.3
-0.4
-0.5
Latitude
50
45
40
35
30
25
-120
-110
-100
-90
-80
-70
Longitude

(c)

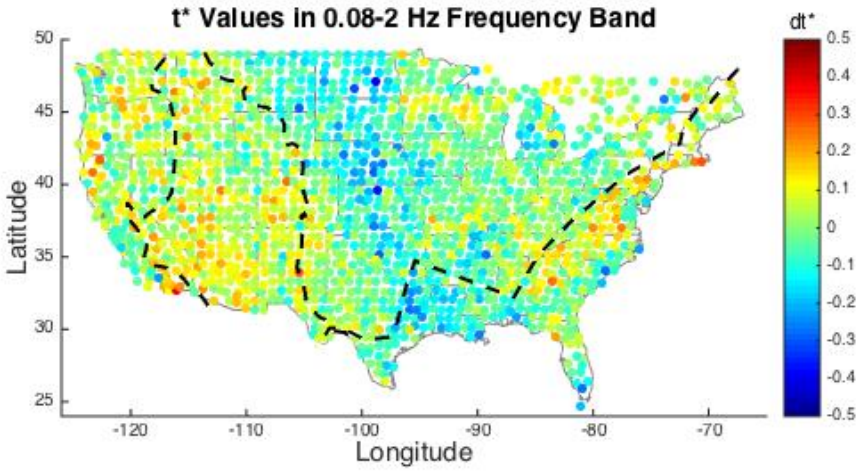

(d)

Figure 10(a-d). Relative *t** maps in the four frequency bands examined. Largest variations appear in 0.08-1Hz band. 0.08-2Hz band map features rough tectonic boundary lines for discussion based on *Whitmeyer and Karlstrom*, 2007**.**

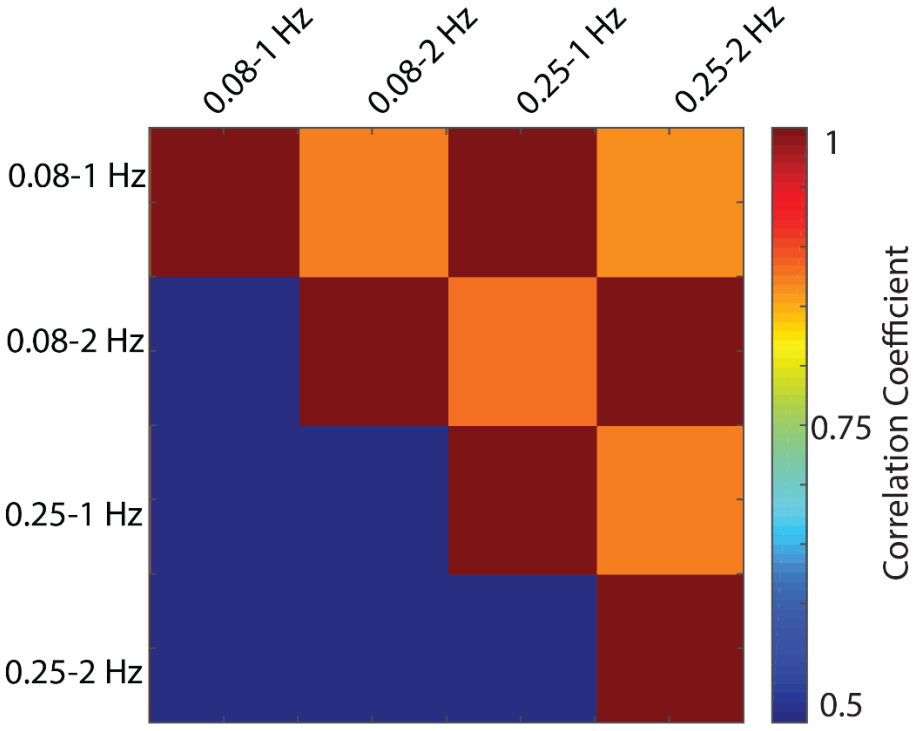

Figure 11. The relationship between different frequency bands is illustrated visually by looking at the correlation coefficients. Correlation values color key on the right. The correlation values are all >0.8.

Many geographic variations are visible across the United States in relative *t** maps (Figure 10). The variations include generally low *t** values in the eastern US and higher values in the western US. The majority of low *t** values are prominent in the central US and run north-south. To better observe the general variations across the continent, various smoothing radii have been applied to the 0.08 – 2Hz d*t** map (Figure 12). General tectonic boundaries have been placed on the smoothed and unsmoothed relative *t** maps for consideration [*Whitmeyer and Karlstrom*, 2007]. For most of the smoothing radii, some of the boundaries between high and low *t** values appear in similar areas as major tectonic boundaries (Figure 10d, Figure 12).

(a)

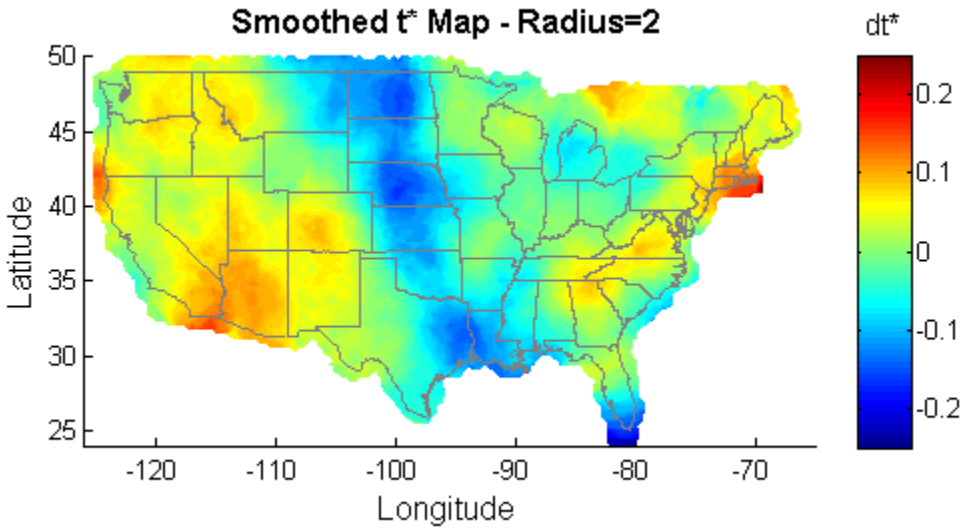

(b)

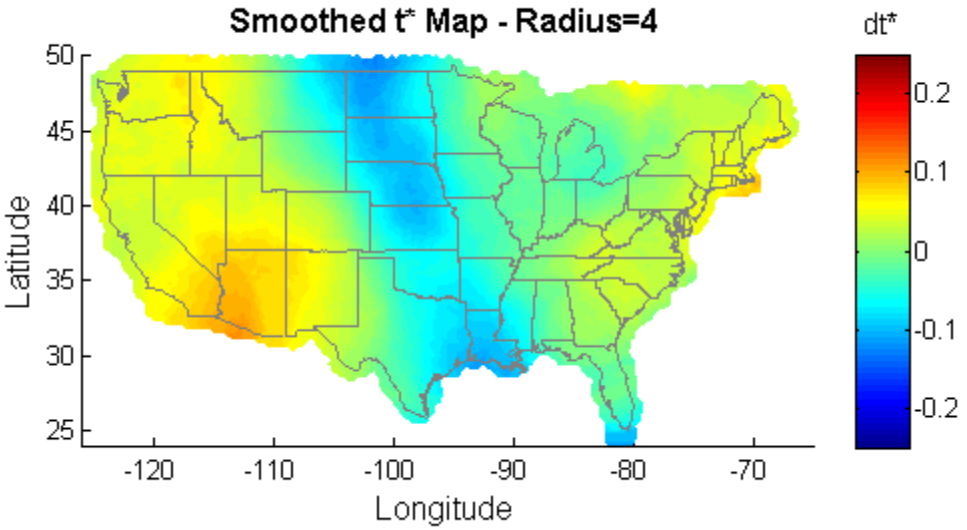
Smoothed t* Map - Radius=4
dt*
0.2
0.1
0
-0.1
-0.2
Latitude
50
45
40
35
30
25
-120
-110
-100
-90
-80
-70
Longitude

(c)

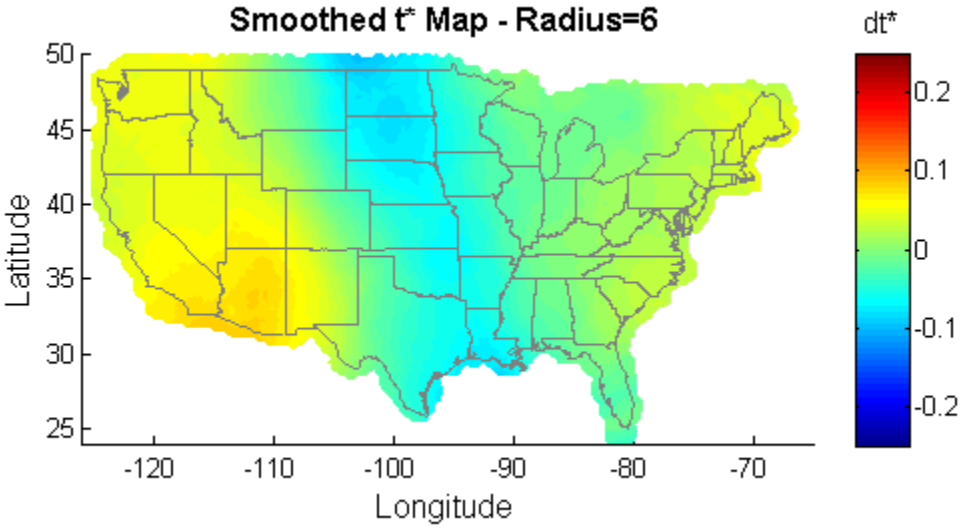
Smoothed t* Map - Radius=6
dt*
0.2
0.1
0
-0.1
-0.2
Latitude
50
45
40
35
30
25
-120
-110
-100
-90
-80
-70
Longitude

(d)

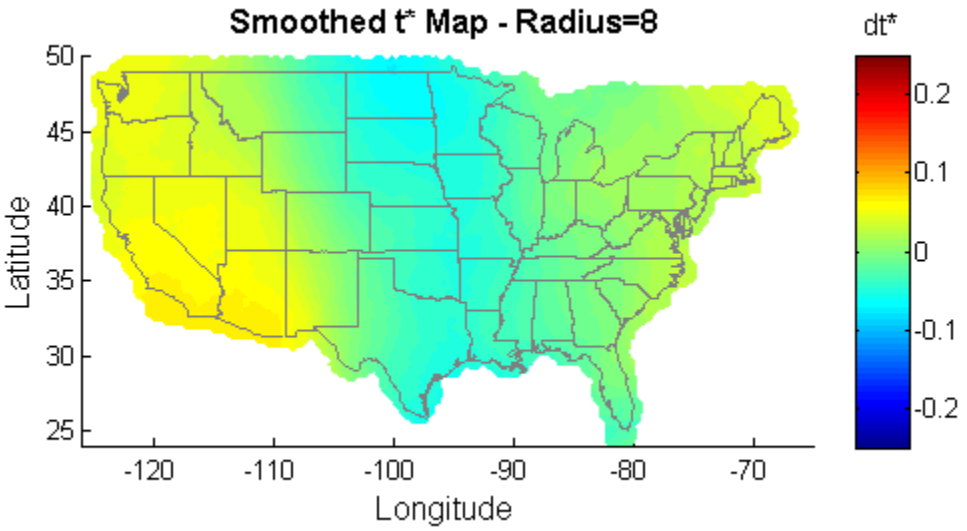

Figure 12(a-d). Smoothed maps of d*t** values derived from spectral ratios with increasing smoothing radii in degrees.

The correlation between the new P wave results and with predictions of *t** from a long period surface wave Q model [*Dalton et al.*, 2008] (Figure 13) were evaluated using a range of smoothing radii between 1 and 12 degrees (Figure 14). When smoothed with a radius of ~8 degrees, relative *t** maps derived from values of absolute Q in a global-scale model in *Dalton et al.*, 2008 show geometries similar to *t** maps derived from EarthScope data: mid to high attenuation values on the west and east coasts and lower attenuation values mid-continent. The correlation value between the abovementioned smoothed map of *t** values from EarthScope data and the map from *Dalton et al.*, 2008 is 0.85 (Figure 14). However, the range of values of unsmoothed relative *t** are larger than *Dalton et al.*, 2008 by one order of magnitude. The values of absolute Q_s from *Dalton et al.*, 2008 were converted to d*t** using the assumptions mentioned in the background. If

the t* results are smoothed with an 8 degree radius, then the difference in magnitude is reduced to ~3x.

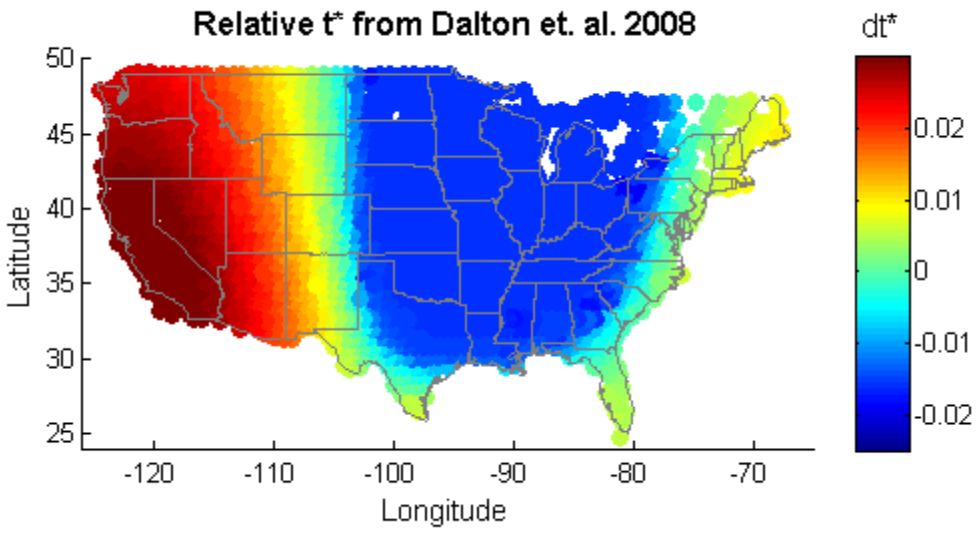

Figure 13. Relative *t** derived from long period surface wave Q model given by [*Dalton et al.*, 2008]. Variations in this map are smooth due to the lateral parameterization of the model in *Dalton et al.*, 2008. Colorbar values are much smaller than those in the d*t** maps developed from EarthScope data.

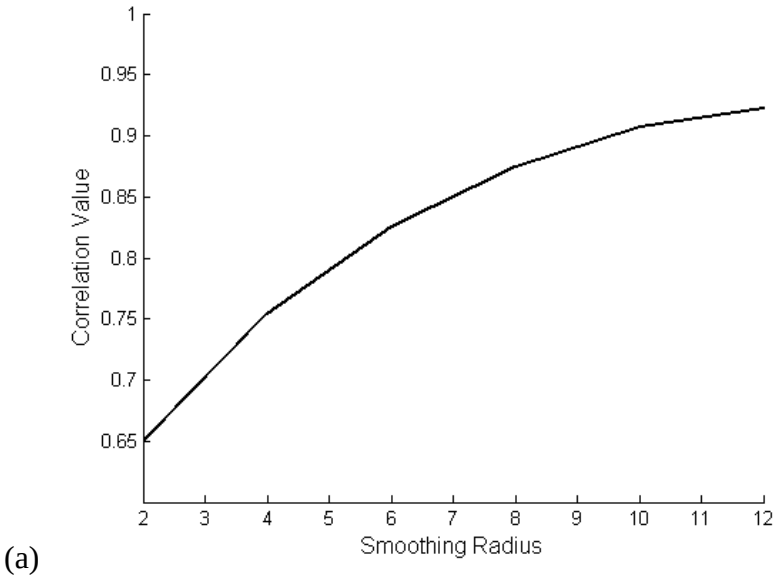

(a)

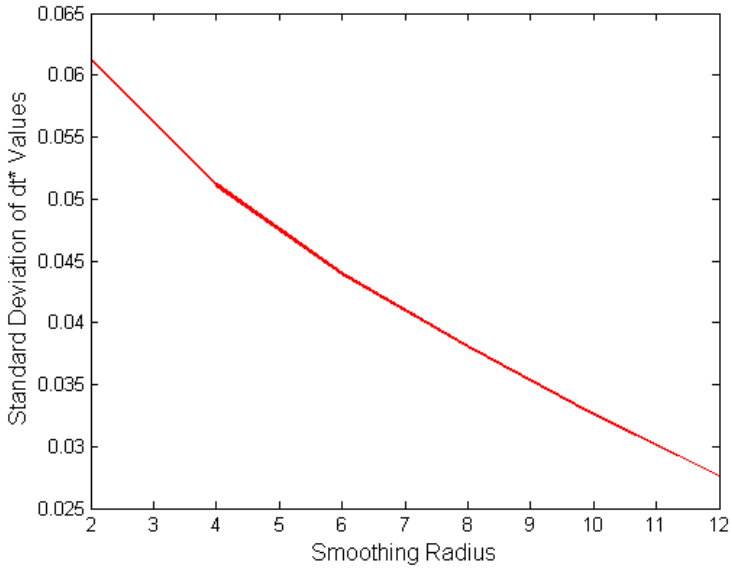

(b)

Figure 14(a-b). Top: Illustration of relationship between smoothing radius and correlation values. Correlation values peak at a smoothing radius of 12 degrees. **Bottom**: Illustration of standard deviations of smoothed d*t** values and the smoothing radii.

For a better understanding of the mechanism of attenuation that is represented by the *t** measurements, the relationship between the transverse and vertical spectra is analyzed. To study how much energy is present on the transverse component, the ratio of

transverse to vertical spectra is plotted (Figure 15) because transverse energy at the time of the P wave represents out-of-plane scattering. The transverse power increases with increases in frequency relative to the vertical power. When the transverse-to-vertical spectral ratio values are binned into quartiles according to t^* value, the greatest transverse-to-vertical ratios are associated with the largest t^* values (Figure 16). Intrinsic attenuation predicts increased power loss with increasing frequency [*Anderson*, 1967]. The results here indicate that loss of energy due to scattering also increases with frequency, and the transverse-to-vertical ratios with the largest positive slopes are correlated with high t^* values. Therefore, scattering that moves vertical energy to the transverse component cannot be easily discriminated from intrinsic attenuation by examining the vertical component spectral ratios of P waves.

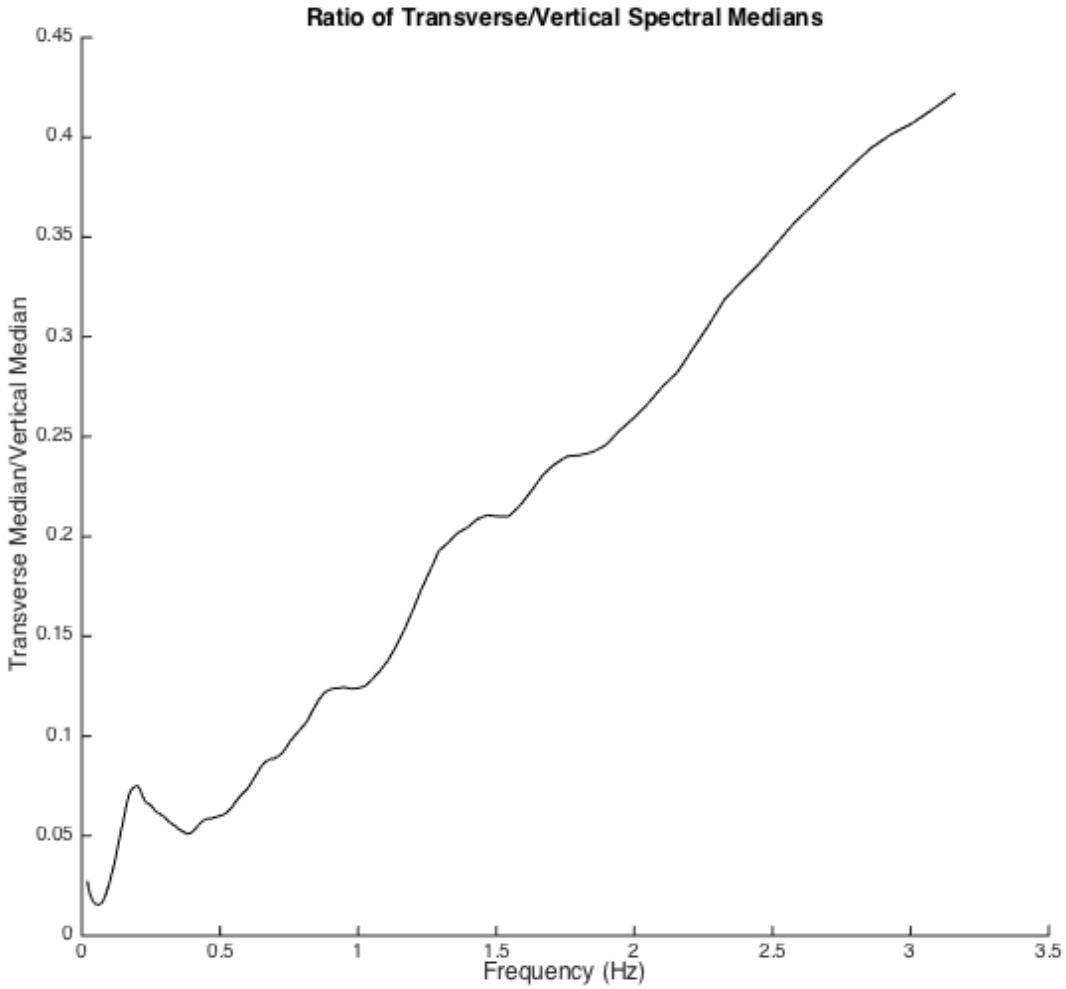

Figure 15. Median transverse-to-vertical ratio over multiple frequencies. A positive slope with increasing frequency is apparent, indicating increasing energy on the transverse component.

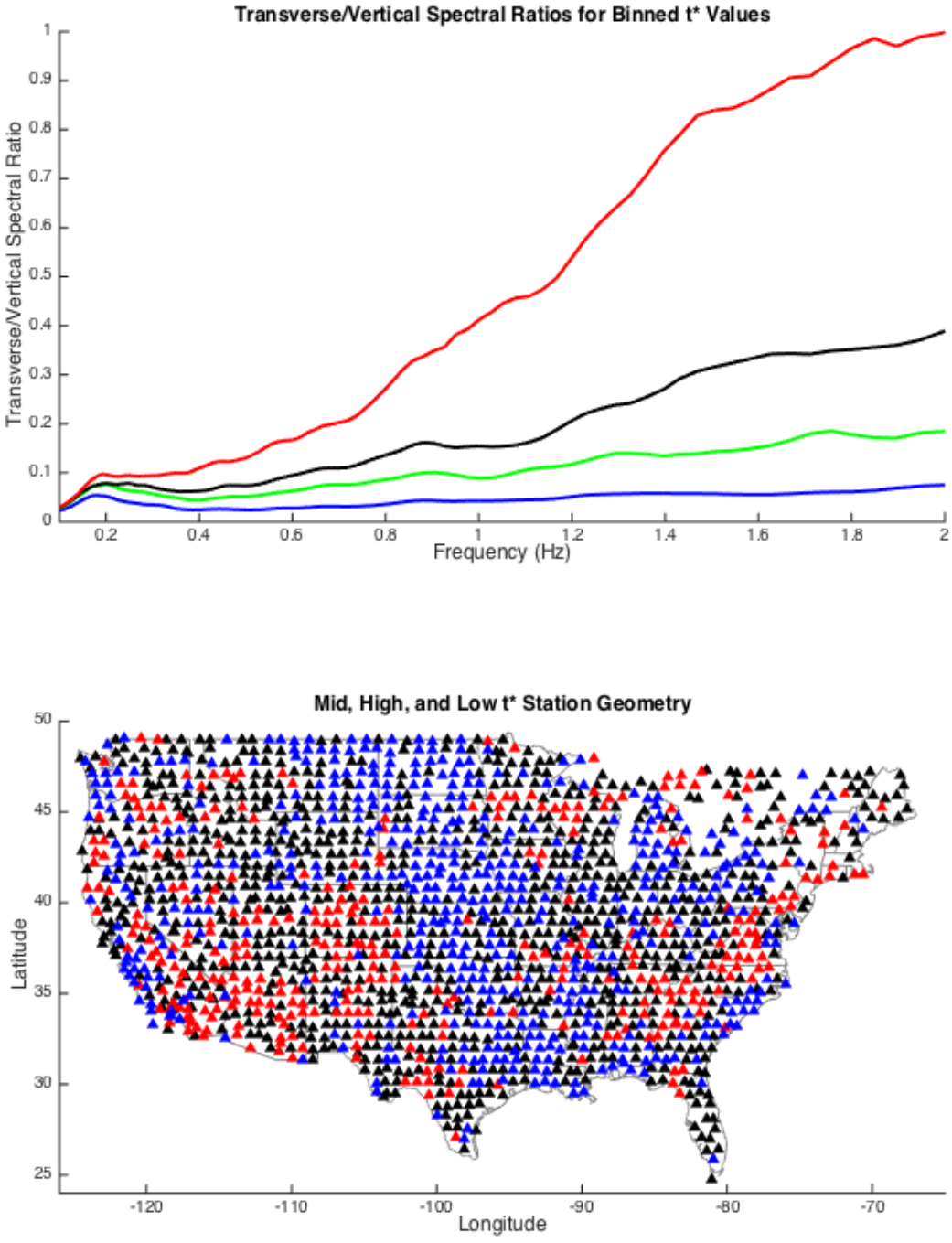

Figure 16. Top: Median transverse-to-vertical spectral ratios for each quartile of *t** values. Red is the highest 25 percent. Black and green are the middle 50 percent. Blue is the lowest 25 percent. **Bottom**: Map of *t** values binned in quartiles. The highest 25 percent are similarly associated with areas of high attenuation in Figure 10d.

6. DISCUSSION

Interpretation of the results points to a number of conclusions. The maps derived from this data explain a number of attenuation features in the upper mantle. In addition, valuable comprehension about the data and experiment process has become apparent through various iterations of data manipulation. For the purposes of discussion and because the correlation between the maps is high, the 0.08-2 Hz frequency band and map will be used (Figure 10d).

5.1 Evaluation of Methods

EarthScope seismic data provide unique high density and wide aperture sampling of continental upper mantle. It is an ideal data set for examining seismic properties beneath the United States. A study of this kind, in which the requirements for the data are so strict, necessitates data with long recording durations. Even though EarthScope spans almost ten years up to this point, the number of Mw>6 deep earthquakes is only 44. These data provide limited azimuthal directions of ray paths. For example, there is only one earthquake due east of the array, and the northeast quadrant of back azimuth direction remains unexplored. It is unclear whether or not this ray geometry has a major effect on the results, but it would be ideal to have a sampling of earthquakes from every direction to obtain azimuthally independent t^* maps or ideally attempt a 3-D inversion for t^*. However, even with limited azimuthal directions, the continental-scale data set has made the results of this study suitable for more robust interpretations than prior studies. If the study had been only in the western US, by example, the attenuation patterns might have been attributed to temperature since the patterns in the western US correlate highly with mantle temperature patterns (Figure 17). However, with some of the unusual

attenuation patterns in the Great Lakes area, Appalachians, and east coast, it can be easily determined that relative *t** patterns are not purely associated with temperature. Instead, the similarly low *t** values in the parts of the Superior craton and Basin and Range provinces indicate that thermal contributions to *t** variations can be overwhelmed by non-thermal effects such as scattering.

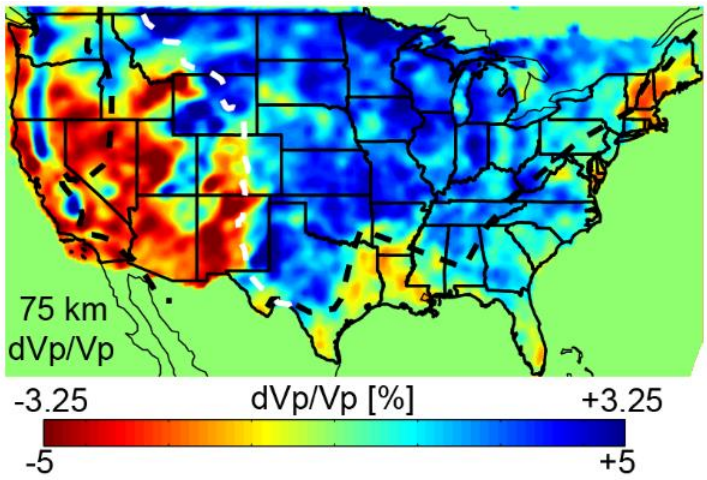

Figure 17. Mantle tomography from P wave velocity data at 75 km depth [*Schmandt and Lin*, 2014]. Dotted white and black lines represent the same major tectonic boundaries from previous figures (Figure 2, Figure 10d).

Optimal frequency bands for this type of study have been determined by examining the data within multiple frequency bands and correlating the results. Despite some noticeable variations in the magnitude within the *t** maps, the correlation values between the four frequency bands in question were high (>0.8) (Figure 11). Above 2 Hz, the signal was typically too weak and those frequencies were less coherent on the vertical component suggesting greater contributions from signal generated noise (e.g. topographic scattering [*Revenaugh*, 1995]).

5.2 Addressing the Magnitude of *t** Variations

Inversion of inter-station P wave amplitude spectra from the Transportable Array provides *t** maps with a previously inaccessible level of resolution and reveals new information about the processes contributing to apparent attenuation in the upper mantle. When comparing the maps from this study to those created after *Dalton et al.*, 2008, a basic observation is that the magnitude of relative *t** values estimated from P wave spectra is about an order of magnitude greater than the predictions from long period surface wave measurements (Figure 18). Though the long wavelength geometries of *t** variations are very similar, an occurrence that will be discussed later, there are a few reasons for the differences in magnitude.

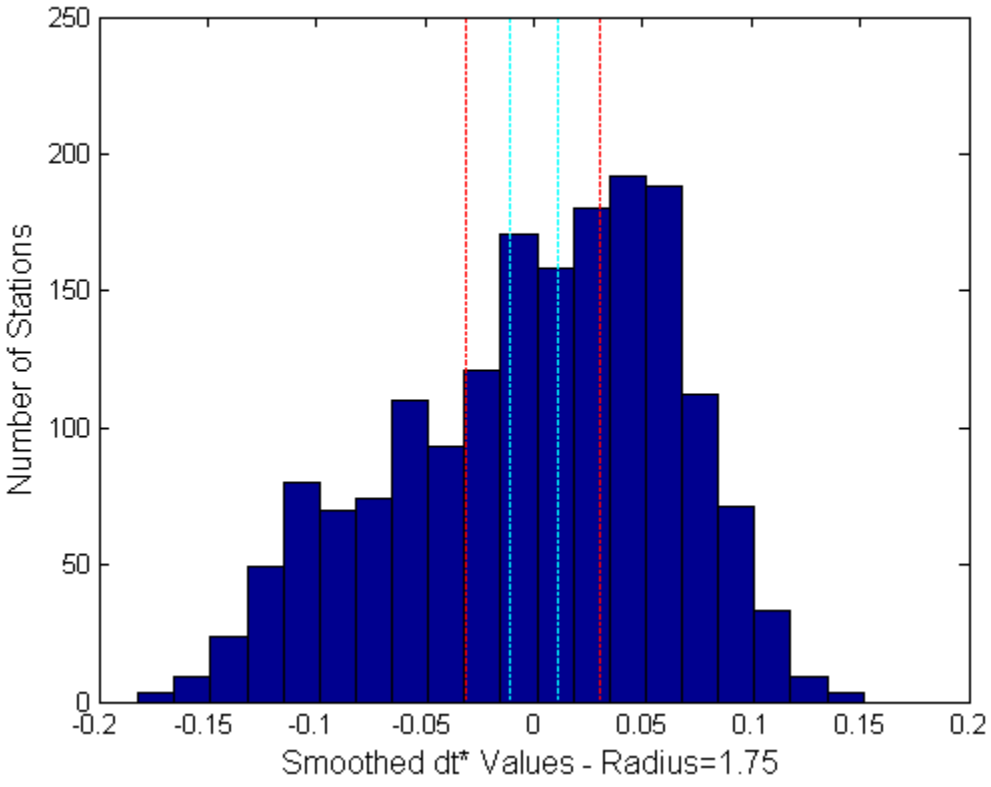

Figure 18. Histogram of relative *t** values for least smoothed map from this study (navy bars); smoothing radius of 1.75 contains about 20 stations averaged at each point. Red

lines indicate global maximum and minimum d*t** values from Dalton using assumptions described in background; cyan bars represent global minimum and maximum from Dalton using slightly different assumptions to illustrate some independence of magnitude difference from conversion values.

The P wave should have negligible power on the transverse component if Earth's seismic structure were 1-D and isotropic. However, the transverse component data from the Transportable Array shows strong energy at the time of the P wave (Figure 4). The presence of this energy points to the potential importance of scattering in redistributing P wave energy in the upper mantle. Heterogeneities in the upper 300 km could break up the wave front and scatter the energy in different directions [*Stein and Wysession,* 2003]. All the energy could still be present, it simply reaches the receivers at different angles causing the appearance of intrinsic attenuation if only the vertical component is analyzed. In Figure 16, the highest *t** values are associated with the largest amount of energy on the transverse component and the steepest transverse-to-vertical ratios for frequencies greater than ~0.4 Hz. These results indicate that high frequency energy loss on the vertical component is largely due to frequency-dependent scattering in addition to any smaller contributions from intrinsic attenuation. Another reason to favor scattering as a more prominent influence on inter-station P wave spectral ratios between 0.08 and 2 Hz is that it provides an explanation for high *t** values observed in areas of cold thick cratonic lithosphere, which cannot be explained by intrinsic attenuation.

5.3 Geographic Variations of *t**

As noted above, the basic geometries of the d*t** maps from both are similar. Most of the high attenuation areas are west of the Rockies and along the Appalachian range.

The high values in the western US also agree with the high relative *t** values in the map derived from *Dalton et al.*, 2008 (Figure 13). High attenuation is intuitive for much of the western US in terms of intrinsic attenuation and scattering; the lithosphere in the western US is relatively thin and warm [*Schmandt and Lin*, 2014]. In addition, the western United States has been tectonically active in recent geologic time [*Whitmeyer and Karlstrom*, 2007]. These high *t** values could be associated with intrinsic attenuation, particularly in the case of the map from *Dalton et al.*, 2008. However, because the western US has seen geologically recent tectonic activity, the tectonic structures present could also contribute to high apparent attenuation values caused by scattering. Suture zones, faults, and volcanism associated with recent compression and extension are examples of wavelength-scale structures could cause the wave front to scatter.

7. CONCLUSIONS

Analysis of P wave attenuation using EarthScope data has provided useful insight into measurable attenuation mechanisms and mantle properties. Despite a relatively low number of total earthquakes, using spectral ratios provides a robust data set with more than 2 million station pairs. Using multiple component P wave amplitude spectra provides a greater understanding of the influence of scattering on overall attenuation patterns. Although there is some frequency dependence of attenuation to be considered, the attenuation patterns seen in the upper 300 km beneath the United States are not sensitive to the choice of bandwidth between 0.08 and 2 Hz. While there are small changes in the magnitude of t^* variations if frequency band is narrowed or widened, the overall geographic patterns remained stable.

The attenuation patterns beneath the United States reveal correlations with temperature and major tectonic structures. These results suggest that areas of high attenuation in the western United States may be associated with both temperature and structure, which would cause intrinsic attenuation and scattering, respectively. Variances in the magnitudes between amplitude spectral ratio studies and long period surface wave Q studies are largely the result of a greater influence from scattering for the higher frequency body wave analysis. The similar geometries of attenuation patterns from spectral ratio studies and Q studies can be explained by the structures that influence scattering: major suture zones, areas of recent deformation, ongoing mantle melting.

Attenuation studies of this type are significant for constraining properties of the mantle and their effects on wave propagation. It is clear that scattering and intrinsic attenuation both contribute to attenuation patterns and must be considered when

interpreting maps for frequencies between 0.08 and 2 Hz. The importance of scattering to P wave amplitude spectra indicates strong elastic heterogeneity in the lithosphere and asthenosphere over length scales of ~5 – 80 km.

8. REFERENCES

Anderson, D. L. (1967), The Anelasticity of the Mantle, *Geophys. J. Int.*, *14*, 135–164.

Cao, A., and A. Levander (2010), High-resolution transition zone structures of the Gorda Slab beneath the western United States: Implication for deep water subduction, *J. Geophys. Res.*, *115*(B7), 1–13, doi:10.1029/2009JB006876.

Dalton, C. a., G. Ekström, and A. M. Dziewoński (2008), The global attenuation structure of the upper mantle, *J. Geophys. Res. Solid Earth*, *113*, 1–24, doi:10.1029/2007JB005429.

Dalton, C. a., G. Ekström, and A. M. Dziewonski (2009), Global seismological shear velocity and attenuation: A comparison with experimental observations, *Earth Planet. Sci. Lett.*, *284*(1-2), 65–75, doi:10.1016/j.epsl.2009.04.009.

Der, Z. a., T. W. McElfresh, and A. O'Donnell (1982), An investigation of the regional variations and frequency dependence of anelastic attenuation in the mantle under the United States in the 0.5-4 Hz band, *Geophys. J. R. Astron. Soc.*, *69*, 67–99, doi:10.1111/j.1365-246X.1982.tb04936.x.

Faul, U. H., and I. Jackson (2005), Grain-size-sensitive seismic wave attenuation in polycrystalline olivine, *Earth Planet. Sci. Lett.*, *234*, 119–134, doi:10.1029/2001JB001225.

Feder, T. (2014), Scoping out the North American continent, 10 years on, *Phys. Today*, *67*(1), 19–21, doi:10.1063/PT.3.2237.

Ford, H. a., K. M. Fischer, and V. Lekic (2014), Localized shear in the deep lithosphere beneath the San Andreas fault system, *Geology*, *42*(4), 295–298, doi:10.1130/G35128.1.

Gilbert, H. (2012), Crustal structure and signatures of recent tectonism as influenced by ancient terranes in the western United States, *Geosphere*, *8*(1), 141–157, doi:10.1130/ges00720.1.

Hammond, W. C., and E. D. Humphreys (2000), Upper mantle seismic wave velocity ' Effects of realistic partial melt geometries, *J. Geophys. Res.*, *105*(B5), 10975–10986.

Hwang, Y. K., J. Ritsema, and S. Goes (2009), Spatial variations of P wave attenuation in the mantle beneath North America, *J. Geophys. Res.*, *114*(B6), B06312, doi:10.1029/2008JB006091.

Hwang, Y. K., J. Ritsema, and S. Goes (2011), Global variation of body - wave attenuation in the upper mantle from teleseismic P wave and S wave spectra, *Geophys. Res. Lett.*, *38*(January), 1–5, doi:10.1029/2011GL046812.

Ingrin, J., and H. Skogby (2000), Hydrogen in nominally anhydrous upper-mantle minerals: concentration levels and implications, *Eur. J. Mineral.*, *12*(3), 543–570, doi:10.1127/0935-1221/2000/0012-0543.

Jackson, I. (2002), Grain-size-sensitive seismic wave attenuation in polycrystalline olivine, *J. Geophys. Res.*, *107*(B12), 1–16, doi:10.1029/2001JB001225.

Karato, S. (2003), Mapping Water Content in the Upper Mantle, in *Inside the Subduction Factory*, pp. 135–152.

Kennett, B. L. N., E. R. Engdah, and R. Buland (1995), Constraints on seismic velocities in the Earth from traveltimes, *Geophys. J. Int.*, *122*, 108–124.

Lee, C.-T. a., P. Luffi, and E. J. Chin (2011), Building and Destroying Continental Mantle, *Annu. Rev. Earth Planet. Sci.*, *39*(1), 59–90, doi:10.1146/annurev-earth-040610-133505.

Lekić, V., J. Matas, M. Panning, and B. Romanowicz (2009), Measurement and implications of frequency dependence of attenuation, *Earth Planet. Sci. Lett.*, *282*(1-4), 285–293, doi:10.1016/j.epsl.2009.03.030.

Lin, F. C., M. H. Ritzwoller, and W. Shen (2011), On the reliability of attenuation measurements from ambient noise cross-correlations, *Geophys. Res. Lett.*, *38*(11), 6–11, doi:10.1029/2011GL047366.

Liu, C., Y. Liu, X. Feng, and Y. Lu (2012), Constructing the convex quadratic function for the evaluation of crack density of HTI media using P- and converted waves, *J. Geophys. Eng.*, *9*, 729–736, doi:10.1088/1742-2132/9/6/729.

Revenaugh, J. (1995), A scattered-wave image of subduction beneath the transverse ranges, *Science*, *268*(5219), 1888–1892, doi:10.1126/science.268.5219.1888.

Romanowicz, B. (1995), A global tomographic model of shear attenuation in the upper mantle, *J. Geophys. Res.*, *100*(B7), 12375–12394.

Schmandt, B., and E. Humphreys (2010), Complex subduction and small-scale convection revealed by body-wave tomography of the western United States upper mantle, *Earth Planet. Sci. Lett.*, *297*(3-4), 435–445, doi:10.1016/j.epsl.2010.06.047.

Schmandt, B., and F. Lin (2014), P and S wave tomography of the mantle beneath the United States, , 6342–6349, doi:10.1002/2014GL061231.Received.

Schmandt, B., K. Dueker, E. Humphreys, and S. Hansen (2012), Hot mantle upwelling across the 660 beneath Yellowstone, *Earth Planet. Sci. Lett.*, *331-332*, 224–236, doi:10.1016/j.epsl.2012.03.025.

Stein, S., and M. Wysession (2003), *An Introduction to Seismology, Earthquakes, and Earth Structure*.

Thomson, D. J. (1982), Spectrum Estimation and Harmonic Analysis, *Proc. IEEE*, *70*(9).

Whitmeyer, S. J., and K. E. Karlstrom (2007), Tectonic model for the Proterozoic growth of North America, , (4), 1–40, doi:10.1130/GES00055.1.